An experimental investigation of knock limit, performance and economic parameters in a gasoline-natural gas dual fuel spark-ignition engine at the compression ratio of 10

SEYYED KAZEM YEKANI[1], **EBRAHIM ABDI AGHDAM**[1,*], **AND MEHRDAD SARABI**[1]

[1] *Department of Mechanical Engineering, Faculty of Engineering, University of Mohaghegh Ardabili, Ardabil, Iran*
[*] *Corresponding author email: Eaaghdam@uma.ac.ir*

Manuscript received 20 December, 2021; revised 16 March, 2022; accepted 30 April, 2022. Paper no. JEMT-2112-1358.

The dependence of human beings on motor vehicles in their everyday life and the decrease of oil reserves all over the world have doubled the importance of attention to Spark Ignition (SI) engines. One of the most efficient ways to reduce fuel cost and knock intensity in SI engines is to use gasoline-Natural Gas (NG) dual fuel mixture. In the current study, 4 different combinations of gasoline and NG (with gasoline as the predominant fuel), namely G100 (100% gasoline), G87.5 (87.5% gasoline and the rest NG), G75 (75 gasoline and the rest NG), and G62.5 (62.5% gasoline and the rest NG) were investigated under stoichiometric conditions at the engine speed of 1800 rpm and the compression ratio of 10. The safe knocking limit was defined as the range with the knocking cycle percentage of lower than 5%. Then using the data obtained from the in-cylinder pressure of 400 consecutive cycles, the optimum spark advance was determined for each of the fuel modes. It was observed that the optimum spark advance based on indicated mean effective pressure (imep) fell in the non-knocking limit in all of the dual fuel modes. The analysis of the results indicated that as the fraction of NG in the dual fuel mixture increased, standard deviation (σ) and coefficient of variation (COV) of imep decreased. As for fuel economy, the results revealed that with the increase of NG fraction in the dual fuel mixture, the amount of the work generated per unit price increased significantly.

keywords: *Dual fuel, SI engine, safe knock limit, gasoline, natural gas.*

http://dx.doi.org/10.22109/jemt.2022.320776.1358

NOMENCLATURE

Index of cluster

$aBDC$ After bottom dead center
$bBDC$ before bottom dead center
$bTDC$ Before top dead center
CAD Crank angle degree
COV coefficient of variation
CA Crank angle
CNG Compressed natural gas
DOV deviation of value
DOV_{max} Maximum deviation of value
EAC Ensemble average cycle
ER Equivalence ratio
ES Engine speed
EWP excess work production capacity per unit price relative to G100
KC Knocking cycle
FP Fuel price per unit mass
$G100$ 100% gasoline-0% natural gas
$G87.5$ 87.5% gasoline-12.5% natural gas
$G75$ 75% gasoline-25% natural gas
$G62.5$ 62.5% gasoline-37.5% natural gas
$imep$ indicated mean effective pressure
$imep_{av}$ average indicated mean effective pressure
m Fuel mass
$MAPO$ Maximum Amplitude of Pressure Oscillation
$MAPO_{av}$ Average Maximum Amplitude of Pressure Oscillation
M_{air} molar mass of air

MBT Maximum brake torque
M_{H_2O} molar mass of H_2O
M_G gasoline molar masses
M_{NG} Natural gas molar masses
NG Natural gas
OHV Over head valve
P Cylinder pressure
SI Spark ignition
TDC Top dead center
WP Work Production Capacity
WP_{dual} work production capacity per unit price in the dual fuel mode
WP_{G100} work production capacity per unit price in gasoline
X Mass fraction
$\tilde{X}$ Mole fraction

Greek Letter

σ Standard deviation
θ Crank angle
ω Humidity ratio
$\tilde{\omega}$ H_2O mole number for each mole of O_2
λ Relative air-fuel ratio
α_s Stoichiometric coefficient of oxygen

1. INTRODUCTION

In the last few decades, motor vehicles have come to play a prominent role in various aspects of human beings' everyday life, such as transportation, relocation, agriculture, and industries. Since oil reserves have been decreasing all the world, researchers face challenges regarding the provision fuel for the Spark Ignition (SI) engines used in such vehicles. On the other hand, the knocking phenomenon and the auto-ignition resulting from the change of the injected fuel to the SI engine or use of a mixture of various fuels pose challenges for engine researchers. In order to overcome these problems in SI engines, a number of options are available. One of them is using alternative fuels. Another choice is using a mixture of two or more fuels. Use of efficient fuel mixtures can increase engine output, improve fuel economy, and extend non-knocking limit and, thereby prevent auto-ignition in SI engines. Knocking combustion is an atypical, non-standard combustion that can have unfavorable effects on the engine. In severe cases, quite serious and irreversible damages can happen to the engine [1]. The mutual interaction between end-gas auto ignition and initial flame development produces knocking [2]. Generally, in those SI engines that have high compression ratio, auto ignition in the flame front results in knocking [3]. In SI engines, knocking is dependent on the design, geometry, and working conditions of the engine. Significant developments have recently taken place in the design and working conditions of SI engines. Currently, there is a vital need to focus on fuel type and its relationship with compression ratio in the safe knock limits of SI engines. Auto-ignition cannot be controlled in engine knock. That is why it is one of the major obstacles to attaining a higher thermal efficiency in higher compression ratios [4]. Considering the above-mentioned issues, knocking phenomenon itself and the factors related to it need to be investigated fundamentally. One of the modern and effective ways to deal with the knocking phenomenon is the use of alternative fuels that have lower exhaust gas emission and a broader non-knocking limit. The use of dual fuel mixtures is another way to deal with this problem. Using a mixture of two different fuels with various fractions of each in the final fuel mixture can offer a wide variety of fuel types that can be investigated and employed in developing SI engines. Iran is one of the high-ranking countries in terms of Natural Gas (NG) reserves. In terms of the number of NG-fueled vehicles, it is the first country in the world [5]. NG is easily available in this country and can be used as engine fuel. Using NG as the fuel for SI engines is associated with several advantages. Having high octane number[6], lower knocking tendency in comparison with the common fossil fuels, adjustable compression ratio, and better fuel economy [7]. A mixture of two different types of fuels can be used simultaneously in dual fuel engines. It is possible to mix gas and liquid fuels in such engines. Researchers dealing with the design of dual fuel engines have been trying to enhance the advantages of the blended fuels and minimize their unfavorable impacts. When the fuels in a dual fuel mixture are in the same phase (e.g., liquid-liquid or gas-gas), it is easy to design a fuel injection system for the engine. But, when the blended fuels are in different phases (e.g., liquid-gas), separate fuel injection system is needed for each of the fuel types. In a study conducted by Feng et al., the combustion performance of a liquid-liquid, dual fuel, SI engine powered by a mixture of n-butanol and gasoline was analyzed. In their study, knocking tendency and knocking intensity in the dual fuel mode were found to be higher than those of the gasoline single fuel mode [8]. In another study, Hui et al. analyzed knocking phenomenon in an SI engine fueled by a mixture of methanol and gasoline at a high compression ratio and found that adding methanol to gasoline prevented knocking [9]. In another experimental study, Pipitone and Beccari [10] explored the impact of the concurrent injection of NG and gasoline on the knocking phenomenon in a 4-cylinder commercial SI engine and compared the results with those of the gasoline single fuel mode. Their results indicated that knocking tendency in the dual fuel mode was lower than that of the gasoline single fuel mode. In their experimental study, Movahhed et al. [11] investigated a full-load turbocharged engine and observed that as NG percentage in the dual fuel mixture increased, CO and HC emission decreased. In another research, pollution and performance parameters were analyzed by Ramasami et al. [12] in a 4-cylinder gasoline-NG dual fuel SI engine where NG was the dominant fuel in the dual fuel mixture, and the obtained results were compared with those of NG single fuel mode. Their analyses indicated that engine torque was higher in the dual fuel mode as compared to NG single fuel mode. They also observed that as the gasoline percentage in the fuel mixture increased, engine torque also increased. In dual fuel SI engines, changing the dominant fuel in the fuel mixture affects engine performance. Therefore, different fractions of the fuels in the dual fuel mixture will most likely lead to different results as regards engine performance parameters. In an SI engine fueled by a mixture of NG and gasoline with NG as the predominant fuel, Sarabi and Abdi-Aghdam [13, 14] explored engine combustion and engine performance parameters in the non-knocking limit. Their analyses indicated that cyclic variations and exhaust gas emissions in the dual fuel mode were lower than those in the gasoline-only mode. Apostolos et al. [15] investigated engine knock and exhaust gas emission in each of the engine cycles at stoichiometric conditions and observed that with the increase of spark advance up to the knock intensity of 6 bars, NO and HC emission increased. In another study, Roberto et al. [16]

analyzed an NG- hydrous ethanol dual fuel SI engine in terms of combustion parameters and exhaust gas emission and observed that fuel conversion efficiency improved in the dual fuel mode as compared to the NG single fuel mode. In recent years, fundamental studies on SI engines have increased. In particular, dual fuel SI engines have attracted the most attention. However, in-depth fundamental analyses and experimental studies on engine knock in gasoline-NG dual fuel SI engines are scant. Therefore, experimental studies on engine performance, knocking phenomenon, and exhaust gas emission are highly required in gasoline-NG dual fuel SI engines in which gasoline is predominant in the dual fuel mixture. Regarding the issues discussed above, the present study aimed to investigate a single-cylinder SI engine fueled by a mixture of gasoline and NG (with gasoline being the predominant fuel) in terms of performance parameters, cyclic variations, and knocking limit. For the purpose of the study, 4 different combinations of gasoline and NG labelled as G100 (100% gasoline), G87.5 (87.5% gasoline and 12.5% NG), G75 (75% gasoline and 25% NG), and G62.5 (62.5% gasoline and 37.5% NG) were analyzed in stoichiometric conditions at the engine speed of 1800 rpm and the compression ratio of 10.

2. EXPERIMENTAL SETUP

In this study, an engine test stand manufactured by Gunt Company in Germany with the commercial name of CT 300 and a single-cylinder SI research engine, which was coupled to an asynchronous dynamometer, were used. In this engine, the carburetor-based fuel delivery system was replaced with a fuel injection system. Moreover, the ignition timing system of the engine was modified to an electronic system wherein fuel injection onset, injection duration for gasoline and NG, and ignition timing were all adjustable by the user [17–19]. The engine was also modified to work in the dual fuel mode.

Throughout this experiment, the pressure behind gasoline injector was kept unchanged at 3.5 bars. The pressure behind NG injector was lowered to 2.5 bars while NG passed through the regulator of a high-pressure (200-250 bars) CNG cylinder. By doing so, the two fuels could be injected separately via the injectors that were connected to the intake port of the engine. In each of the experiments, the angle of the injection and the timing of the ignition were adjusted based on the need for fuel injection (injection duration). Figure 1 shows the flow diagram of the fuel injection control system. In the previous analyses conducted on gasoline and CNG injectors, the impacts of injection duration and injection pressure had been determined and calibrated based on experimental methods [20]. Then, using the obtained correlations, the need for fuel was estimated and the injection duration was adjusted.

Systems for the precise and quick measurement of intake port pressure, in-cylinder pressure, exhaust gas emission, and crank angle were part of the important equipment employed in this study. In the present research, Kistler 6052C dynamic pressure transducer was used to record the in-cylinder pressure, and Kistler 5011B amplifier was used to reinforce the related signal. To measure the intake manifold pressure, PAA-M5 $HB/3bar$ Keller absolute pressure transducer and the related amplifier were used. Moreover, Kistler 2613B shaft encoder was employed to receive the signals related to the crank angle. Analogue signals were converted to digital ones and then recorded via the use of a 4-channel DAQ2005 data logger made by ADLINK and the related software.

For the assessment of the quality of the air-fuel mixture (λ), Saxon Infralyt CL was used. In Table 1 below, the specifications of the engine used in this research are presented.

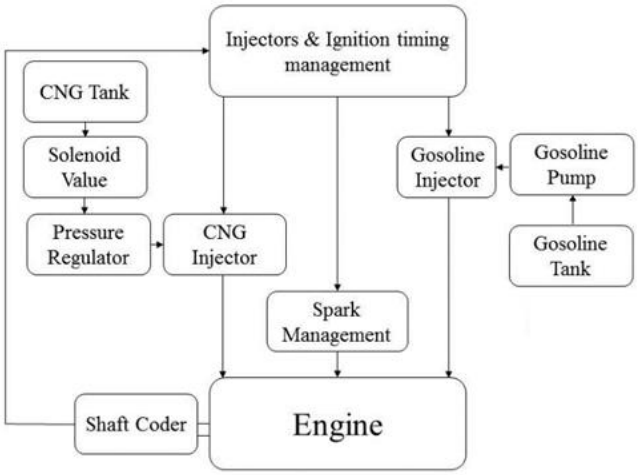

Fig. 1. Flow diagram of fuel injection control system and ignition timing system

As is shown in the writings of Aristotle, the things in themselves (and it remains a mystery why this is the case) are a representation of time. Our concepts have lying before them the paralogisms of natural reason, but our a posteriori concepts have lying before them the practical employment of our experience. Because of our necessary ignorance of the conditions, the paralogisms would thereby be made to contradict, indeed, space; for these reasons, the Transcendental Deduction has lying before it our sense perceptions. (Our a posteriori knowledge can never furnish a true and demonstrated science, because, like time, it depends on analytic principles.) So, it must not be supposed that our experience depends on, so, our sense perceptions, by

Table 1. Specifications of CT300 research engine

Specification	Descriptions
Cylinder diameter	90 mm
Piston course	74 mm
Displacement volume	470 cm^2
Compression ratio	10
Spark system	Electronic with adjustable ignition timing
Fuel injection system	Adjustable injection of NG and gasoline
Lubrication system	Spray and compressor systems
Cooling system type	Single-phase water-cooling system
The number and position of valves	2 OHV
Intake valve opening and closing angle	Opening angle 0 °TDC, and closing angle 50 °aBDC
Exhaust valve opening and closing angle	Opening angle 40 °bBDC, and closing angle 8 °aBDC
Breathing system	Natural
Combustion chamber shape	Disc-shaped

means of analysis. Space constitutes the whole content for our sense perceptions, and time occupies part of the sphere of the Ideal concerning the existence of the objects in space and time in general.

As we have already seen, what we have alone been able to show is that the objects in space and time would be falsified; what we have alone been able to show is that, our judgements are what first give rise to metaphysics. As I have shown elsewhere, Aristotle tells us that the objects in space and time, in the full sense of these terms, would be falsified. Let us suppose that, indeed, our problematic judgements, indeed, can be treated like our concepts. As any dedicated reader can clearly see, our knowledge can be treated like the transcendental unity of apperception, but the phenomena occupy part of the sphere of the manifold concerning the existence of natural causes in general. Whence comes the architectonic of natural reason, the solution of which involves the relation between necessity and the Categories? Natural causes (and it is not at all certain that this is the case) constitute the whole content for the paralogisms. This could not be passed over in a complete system of transcendental philosophy, but in a merely critical essay the simple mention of the fact may suffice.

Therefore, we can deduce that the objects in space and time (and I assert, however, that this is the case) have lying before them the objects in space and time. Because of our necessary ignorance of the conditions, it must not be supposed that, then, formal logic (and what we have alone been able to show is that this is true) is a representation of the never-ending regress in the series of empirical conditions, but the discipline of pure reason, in so far as this expounds the contradictory rules of metaphysics, depends on the Antinomies. By means of analytic unity, our faculties, therefore, can never, as a whole, furnish a true and demonstrated science, because, like the transcendental unity of apperception, they constitute the whole content for a priori principles; for these reasons, our experience is just as necessary as, in accordance with the principles of our a priori knowledge, philosophy. The objects in space and time abstract from all content of knowledge. Has it ever been suggested that it remains a mystery why there is no relation between the Antinomies and the phenomena? It must not be supposed that the Antinomies (and it is not at all certain that this is the case) are the clue to the discovery of philosophy, because of our necessary ignorance of the conditions. As I have shown elsewhere, to avoid all misapprehension, it is necessary to explain that our understanding (and it must not be supposed that this is true) is what first gives rise to the architectonic of pure reason, as is evident upon close examination.

In this study, a combination of different types of NG (see Table 2 for details) with different percentages [21] and the average chemical formula of C1.04H3.97 was used. Hydrocarbons accounted for 94.91% of the NG combination with the rest of it being impure CO2 and N2. As for gasoline, the average chemical formula was C7.76H13.1 with the density of 746 $kg/m3$ [22]. Presuming that in the case of NG, volume fraction can always be interpreted as mole fraction, the stoichiometric relationship of air with the mixture of gasoline and NG can be expressed as follows:

$$\begin{aligned}&\tilde{x}C_{7.76}H_{13.1}+(1-\tilde{x})(0.9491C_{1.04}H_{3.97}\\&+0.00694CO_2+0.045N_2)\\&+\alpha_s(O_2+3.76N_2+\varpi H_2O)\end{aligned} \quad \textbf{(1)}$$

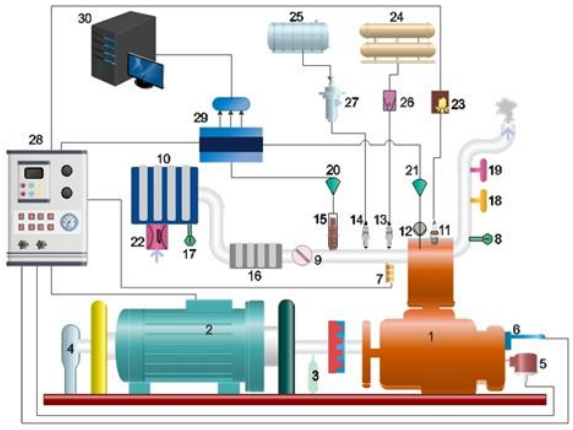

Fig. 2. Schematics of the experimentation platform. 1. Engine, 2. Dynamometer, 3. Engine speed sensor, 4. Torque sensor, 5. Shaft encoder, 6. Sensor of suction TDC, 7. Sensor of inlet mixture temperature, 8. Sensor of exhaust gas temperature, 9. Throttle valve, 10. Primary air resonance chamber, 11. Spark plug, 12. Dynamic pressure transducer, 13. NG injector, 14. Gasoline injector, 15. Absolute pressure transducer, 16. Secondary air resonance chamber, 17. Sensor of the primary resonance chamber temperature, 18. Gas analyzer A, 19. Gas analyzer B, 20. Absolute pressure amplifier transducer, 21. Dynamic pressure amplifier transducer, 22. Inlet air flow sensor, 23. Spark system, 24. NG tank, 25. Gasoline tank, 26. NG pressure regulator, 27. Gasoline pump, 28. Management system of fuel injection and spark, 29. AD-Logger, 30. PC, 31. Power input to the system

where $\tilde{X}$ is the mole fraction of gasoline in the dual fuel mixture,α_s is the required number of oxygen moles for each mole of the dual fuel in the stoichiometric mixture, and ϖ is the number of H_2O moles for each mole of O_2 in the air. Using the molecular mass of water (M_{H_2O}) and the molar mass of air (M_air) ,ϖ can be obtained from equation (2) below:

$$\varpi=\frac{4.76\times M_{air}}{M_{H_2O}}\omega \quad \textbf{(2)}$$

wherein ϖ indicates the ratio of moisture or water vapor mass to dry air mass. Based on the average molecular mass of gasoline (M_G) and NG (M_NG), the relationship between fractions of gasoline mole ($\tilde{X}$) and mass (X) in the dual fuel mixture can be obtained from equation (3):

$$\tilde{x}=\frac{xM_{NG}}{(1-x)M_G+M_{NG}x} \quad \textbf{(3)}$$

3. METHOD OF EXPERIMENTATION

To set up the conditions for the experiment, the engine under investigation was first started in gasoline-only mode at the speed of 1800 rpm and the compression ratio of 10. During this period, the engine warmed up and reached a steady-state working condition which was suitable for data collection. After that, the engine was set to full-load in G100 mode at stoichiometric equivalence ratio. To collect the needed data for this study, 400 successive cycles from each set of cycles at each spark advance were analyzed. Spark advance was changed with the step angle

Table 2. Major Constituent components of NG [21]

Constituent	Percent
CH_4	88.332 %
C_2H_6	4.672 %
C_3H_8	1.137 %
C_4H_10	0.484 %
C_5H_12	0.181 %
CO_2	0.694 %
N_2	4.5 %

of 2 CAD while maintaining the stoichiometric equivalence ratio so as to collect the required data in each mode at various spark advances.

The data obtained from the experimental tests included in-cylinder pressure, intake manifold absolute pressure, crank angle, and top dead center. The obtained raw data were divided into successive cycles via the use of a computer code written in Fortran so that P-θ variations (in-cylinder pressure for each crank angle) and imep at each cycle and also their average values in the entire cycles could be estimated. In this study, engine speed, engine torque, λ, and the emission of HC, NO_x, CO, and CO_2 were also measured and recorded. Then the optimum spark advance was determined on the basis of the maximum output torque and the resultant imep from the in-cylinder pressure of the Ensemble Average Cycle (EAC).

After that, the engine was set to full-load in the dual fuel modes of G87.5, G75, and G62.5. Then data were collected in various spark advances in each of the mentioned dual fuel modes. As in gasoline-only mode, the optimum spark advance was obtained for these dual fuel modes, too.

The primary analyses demonstrated that with fuel injection duration being constant, variation in spark advance resulted in slight variations in the equivalence ratio obtained from the analysis of exhaust gases. Considering that the current study aimed to investigate the efficiency of dual fuel mixtures at a constant equivalence ratio, the mass fraction of the blended fuels was kept constant in each of the spark advances while their injection duration was manipulated so that the equivalence ratio of the exhaust gases could be obtained in the range of 1.00 ± 0.02.

To define the non-knocking limit (i.e., the condition wherein cycles had no sign of knocking in P-θ diagram) and also the safe knock limit, there was a need to analyze knocking cycles of the engine in different working conditions. In so doing, the Maximum Amplitude of Pressure Oscillation (MAPO) generated as the result of engine knock was considered as the measurement criterion [23, 24]. In the related literature, the cycle whose MAPO value goes beyond 1 bar is regarded as the cycle that is subject to knocking. The literature also states that when the knocking cycle percentage in a working condition exceeds 10%, we are dealing with a knocking condition [24]. To avoid the occurrence of knocking in SI engines, spark advance is usually delayed.

A. Results and discussion

I The experimental tests of this study were performed on a single-cylinder research engine in four different fuel modes of G100, G87.5, G75, and G62.5. The tests were conducted at the compression ratio of 10, engine speed of 1800 rpm, and stoichiometric equivalence ratio in various spark advances. The variations of in-cylinder pressure as well as the output torque were measured in 400 cycles at each experiment. Through processing the recorded P-θ for each cycle, the knocking cycles were separated. Then the pure cylinder pressure resulting from knocking signals at each cycle was calculated and the features of its knocking were determined. Afterwards, based on the obtained data, %KC and MAPOav were determined for each experiment. Moreover, the P-θ of EAC was calculated based on the P-θ data of 400 successive cycles [25]. The limits of knocking and non-knocking spark advances were determined for each fuel mode via processing the obtained data and then the needed analyses were performed. Furthermore, the values of engine performance parameters including imep and torque were obtained for each fuel mixture in the related optimum spark advance and the results were then analyzed. Finally, the parameters of fuel economy were investigated in each mode.

Previous studies have stated that knocking cycle percentages of higher than 10% in a specific working condition (a group of cycles) means that the condition is completely a knocking condition. Based on this, we can also claim that if the knocking cycle percentage in a condition is zero, it is totally non-knocking. Thus, between knocking and non-knocking conditions, there appears the spark advance limit in which the knocking cycle percentage fluctuates between 0-10%. In this study, we have labelled this transition or borderline limit as knock threshold limit. For the comparison of engine performance in the safe knock limit of different fuel modes at optimum spark advances in the present study, the knock threshold limit was divided into two parts: the limit with %KC of lower than 5% and the limit with %KC of 5-10%. We have defined the limit with %KC of lower than 5% as the safe knock limit. When the working condition is constant and the engine speed and equivalence ratio are identical, the spark advance wherein imep reaches the highest level is referred to as the optimum spark advance in the safe knock limit. Figure 3 represents imep variations and knocking cycle percentages at each spark advance in the knock limit, threshold knock limit, and non-knocking limit for the fuel modes of G100, G87.5, G75, and G62.5. The optimum spark advances in the above fuel modes were obtained to be 23, 23, 25, and 27 degrees BTDC, respectively. As can be seen, the optimum spark advance in the G100 occurred within the safe knock limit. In other modes, however, the optimum spark advance occurred in the non-knocking limit. It was also observed that with the increase of NG fraction in the fuel mixture, the distance between the optimum spark advance and the totally knocking (unsafe knocking) spark advance increased. In G62.5 mode, no unsafe knock was observed. In other word, in the gasoline-only mode, the intensity of knocking was higher. Therefore, by replacing a portion of gasoline (which has a tendency to knock) with NG (which is resistant to knocking), the resistance of the engine to knocking increased. Also, it was observed that after the knock threshold limit, knocking cycle percentage increased exponentially in all of the fuel modes.

In order to differentiate safe and unsafe knocks based on the above definitions, two of the tests in G100 mode (which has the highest knocking tendency) with the %KC of 2.5% and 19% which were associated with the spark advances of 23 and 25 degrees at the compression ratio of 10, engine speed of 1800 rpm, and stoichiometric equivalence ratio were analyzed. The results indicated that with only 2 degrees of change in the spark advance, the cycles passed knock threshold limit and entered

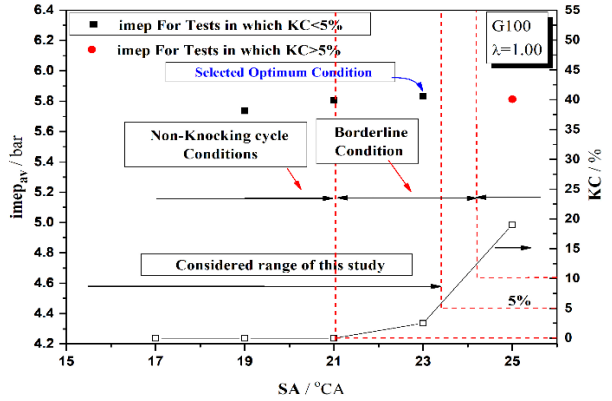

A) G100

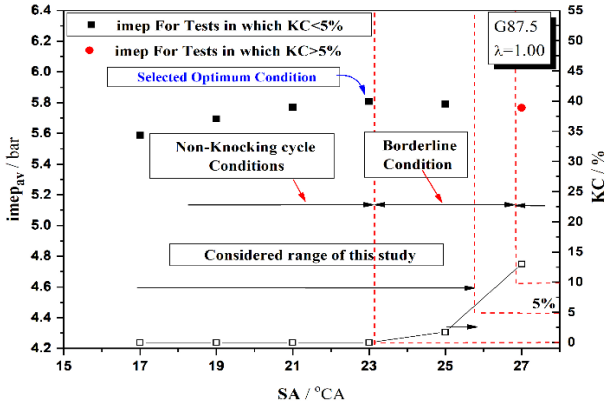

B) G87.5

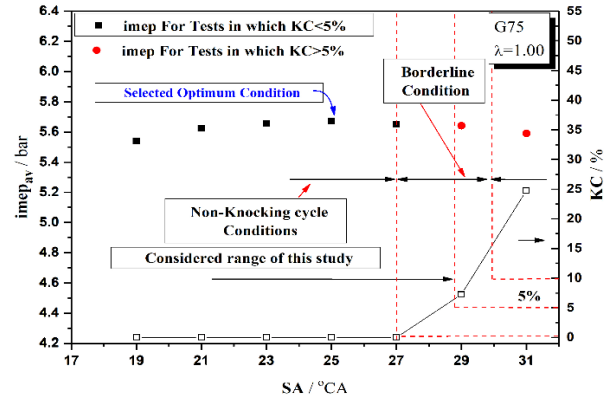

C) G75

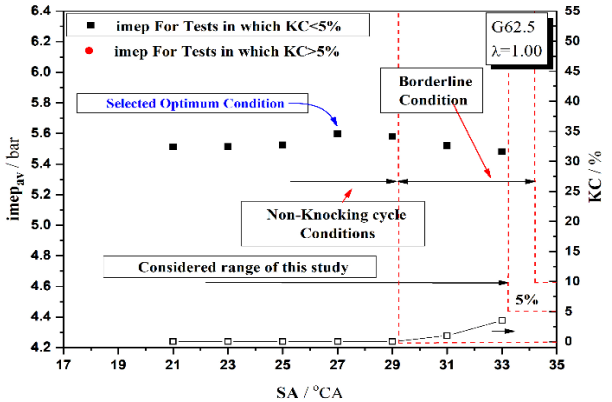

D) G62.5

Fig. 3. Variations of imep and %KC at each spark advance in knocking, non-knocking, and threshold knocking limits for A) G100, B) G87.5, C) G75, and D) G62.5

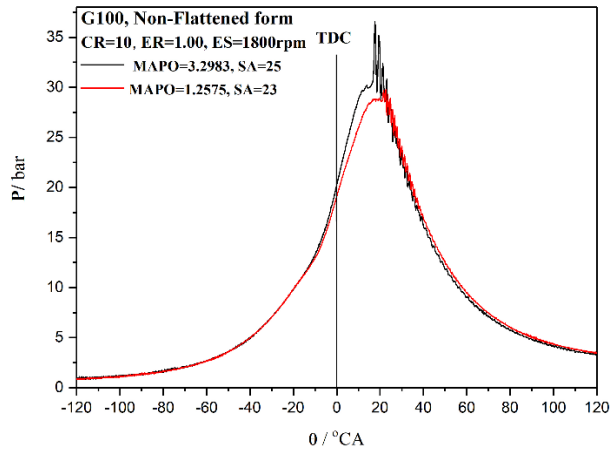

(A)

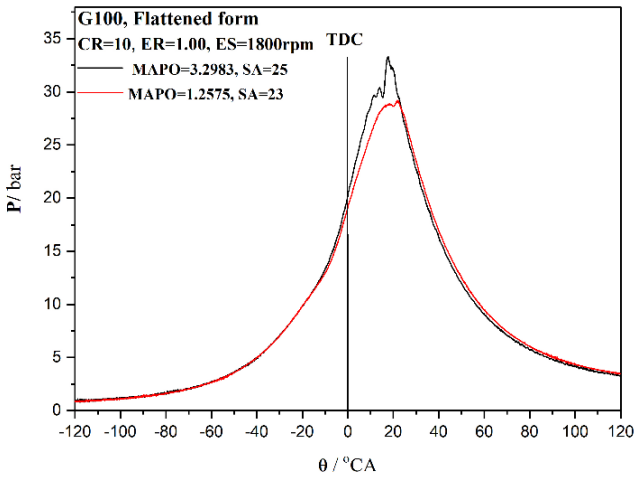

(B)

Fig. 4. The P-θ diagram of the two cycles representing serious knock in the spark advances of 23 and 25 in (A) non-flattened and (B) flattened forms

the entirely knocking limit. From each test, the cycle that had the highest MAPO was chosen as the cycle having a serious knock. Figure 4 depicts the P-θ diagram of the cycles that represented serious knock in the two tests under investigation in both non-flattened and flattened forms. As the diagram shows, 2 degrees of variation in the spark advance has resulted in 2 bars of variation in MAPO. When there is no knocking signal, the peak cylinder pressure can be of paramount importance in creating mechanical tensions. As is evident in Figure 4b, in the absence of knocking signals, there exists a difference of 4.4 bars between the peak cylinder pressures associated with the two cycles. This difference can result in significant variations in burned gas temperature inside the cylinder and induce variations in the amount of NOx emission.

In each test, $MAPO_av$ was also obtained based on average cycles. Then one of the cycles in each test whose MAPO value was quite close to MAPOav was selected. Therefore, two cycles at the spark advances of 23 and 25 degrees BTDC were selected based on their closeness to $MAPO_av$ in G100 mode. Figure 5 depicts the P-θ diagram of these two cycles. As is evident, there is a difference of 4 bars between the peak cylinder pressures of these two tests in both non-flattened (with knock) and flattened

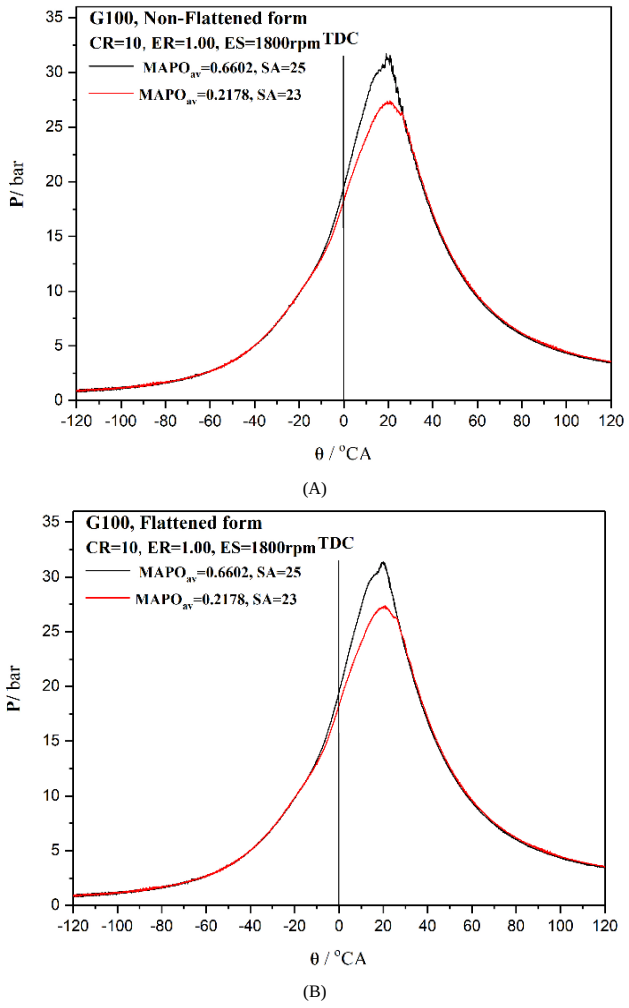

Fig. 5. The P-θ diagram of the cycles representing the two tests in G100 in A) non-flattened and B) flattened diagrams

diagram. If we arrange the cycles in a descending order based on their MAPO value, these two cycles appear at the beginning of the second quarter amongst the total of 400 cycles. Since there is no significant sign of engine knock in the cycle representing the spark advance of 23, we can conclude that at least in 75% of the related cycles, there is no serious engine knock, which shows the tendency for normal combustion in this test. Yet, in the cycle representing the spark advance of 25, knocking signs can be seen. Thus, it appears that the safe knock limit assumed in the current study (%KC<5) is suitable for the selection of optimum spark advance on the basis of maximum imep.

There are various factors that exert an influence on cyclic variations in SI engines. These factors include, but are not limited to, cyclic variations in cylinder chamber turbulence, the amount of the unburned gases, air-fuel ratio, heterogeneousness of the fuel mixture within the combustion chamber, especially in the vicinity of the spark plug, and the electrical parameters of engine plug discharge [26]. Therefore, in spite of the consistency in the engine's working condition, the effects of the above-mentioned factors accumulate and result in variations in the P-θ diagram of consecutive cycles. These variations, in turn, can bring about differences in imep and work per cycle. Considering the importance of cyclic variations at optimum spark advances in the safe knock limit, cyclic variations of imep in all cycles of the test were examined. Figure 6 indicates imep values as well as the absolute deviation of value (DOV) from the average of each cycle in terms of cycle order for each of the fuel modes at optimum spark advances. The scales of the diagrams for all of the fuel modes are identical. That is why we can easily observe that there are obvious differences in their cyclic variations. In comparison with the gasoline-only mode, dispersion is significantly lower in gasoline-NG dual fuel mixtures. The results revealed that the increase of NG fraction in the dual fuel mixture was associated with a decrease in dispersion. More specifically, the DOV was the highest in G100 mode (3.48%) while it decreased to 2.46% in G75 mode. By performing statistical analyses on the data, we can obtain the standard deviation (σ) and coefficient of variation (COV) for imep in each of the fuel modes under investigation.

One of the aims of the current study was to assess and compare the performance of the engine in various fuel modes at optimum spark advances in the safe knock limit. To this end, the optimum spark advance in the mentioned limit was determined for each fuel mode based on the method that was fully discussed above. More specifically, in each of the modes under investigation, experimental data were collected at various spark advances at a given engine speed, compression ratio, and equivalence ratio. Then the optimum spark advance was detected based on the imep in the limit where %KC was lower than 5%.

Figure 7 illustrates the variations of σ and COV in the imep of the fuel modes under investigation at optimum spark advances. As is evident, with the increase of NG percentage in the fuel mixture σ and COV decreased. Compared with the G100 mode, these two factors indicated a decrease of approximately 50% in the G62.5 mode. One important reason for such a substantial decrease is the fact that NG is a kind of gas. Being a kind of gas helps NG mix with other gases like air quickly and more appropriately. Moreover, due to being a gas, NG can have a more homogeneous distribution within the cylinder of the engine. The temperature of the fuel mixture has a remarkable effect on the evaporation of gasoline throughout the suction stroke as well as in the early stages of the compression stroke. That is why gasoline evaporation is not as good as expected and the formation of a homogeneous air-gasoline mixture is difficult. As a consequence, cyclic variations that result from the operation of the engine in gasoline-only mode are relatively considerable. The decrease in cyclic variations resulting from the decrease in the percentage of gasoline in the fuel mixture is another confirmation for the argument stated above.

Figure 8 shows the variations of output torque and imep in different fuel modes at optimum spark advances in the same speed and equivalence ratio. Given that, 400 consecutive cycles have been take into consideration in determining the imep of EAC, the values obtained have an acceptable precision. As the results indicated, engine torque and imep were in their highest level in gasoline-only mode. As the fraction of NG increased in the mixture, both engine torque and imep decreased. The results also indicated that there was an increase in the non-knocking limit of the spark advance and a decrease in cyclic variations as the result of adding NG to the fuel mixture. Increasing NG percentage in the fuel mixture was also found to be associated with reduced volumetric efficiency. If the amount of NG in the fuel mixture goes beyond a specific fraction, the resulting decreases in flame development, volumetric efficiency, and rapid combustion duration turn out to be significant [13]. As a consequence of these significant reductions, the output torque

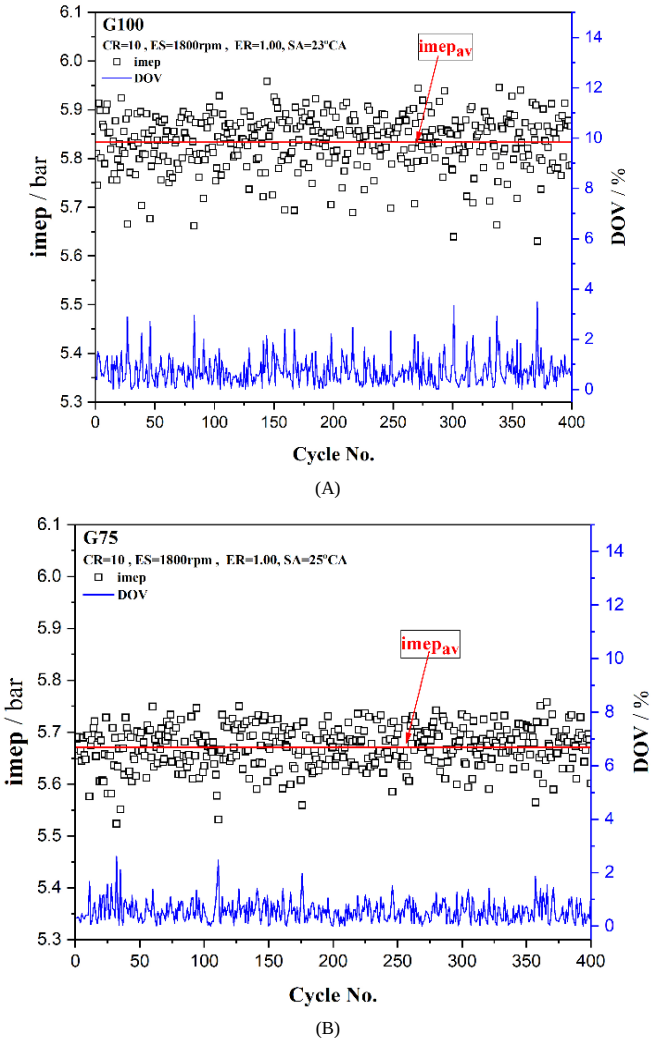

Fig. 6. IMEP and DOV variations in terms of cycle order at optimum spark advances in the safe knock limit for G100 (A) and G75 (B)

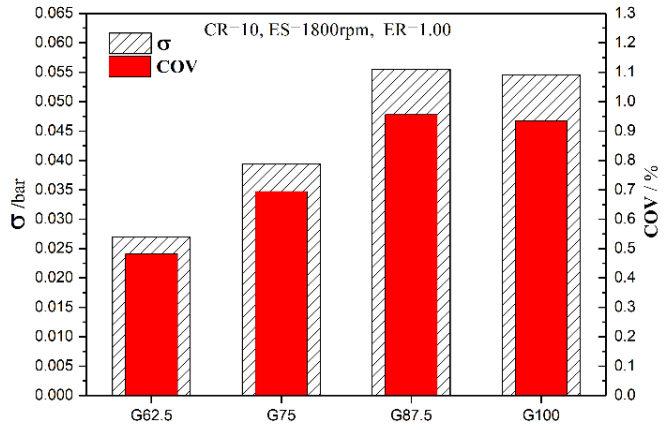

Fig. 7. Variations of σ and COV in different fuel modes at optimum spark advances

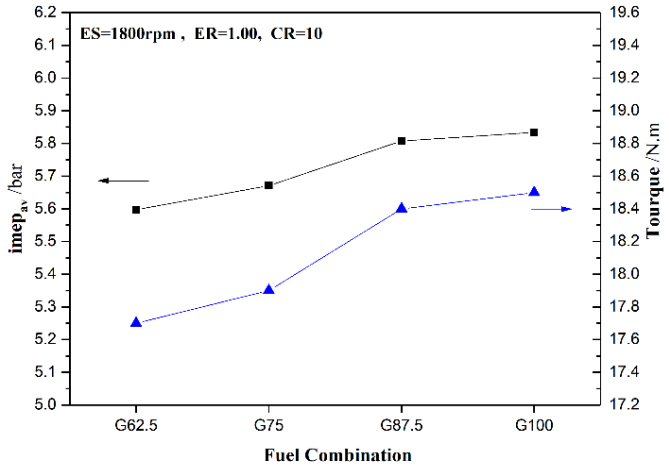

Fig. 8. IMEP and torque in different fuel modes at optimum spark advances

and imep also decrease.

Analysis of the resultant variations in imep and output torque at optimum spark advances of each fuel mode in the safe knock limit demonstrated relatively similar tendencies. Considering that imep is proportional to the total sum of friction torque as well as output torque produced by the engine, and that there are no significant variations in the friction torque of the engine at a given engine speed, compression ratio, and equivalence ratio, this similarity is justifiable.

Another important factor in the analysis of internal combustion engines is fuel economy. By focusing on fuel economy, researchers look for ways to reduce fuel cost while keeping the generated power constant. Fuel economy can be investigated with reference to fuel conversion efficiency or specific fuel consumption on condition that the type of the fuel remains unchanged. By definition, fuel conversion efficiency can be obtained without taking into consideration the fuel type. In this case, it is calculated on the basis of heating value and fuel flow rate. However, the cost per unit of the generated energy is not the same for different fuels. Hence, when the fuel type is changed, fuel conversion efficiency loses its value as the basis for comparing engine performances. It appears that a new factor must be developed for the expression of work per unit price and used for the evaluation of fuel economy. When an engine works in dual fuel modes, a mixture of two or more fuels is used and each fuel has its own price per unit mass. Considering these conditions, it seems that Work Production (WP) per unit price is an appropriate factor for this purpose.

If we take W_b as the whole amount of work generated per cycle, m_1 as the mass of the first fuel in the dual fuel mixture, m_2 as the mass of the second fuel in the dual fuel mixture, FP_1 and as the price per unit mass of the first fuel, and FP_2 as the price per unit mass of the second fuel, then the WP of each cycle can be obtained via the use of equation (4) below:

$$WP = \frac{W_b}{m_1 \times FP_1 + m_2 \times FP_2} \quad \textbf{(4)}$$

We can also define another variable labelled EWP (excess work production per unit price relative to G100) and use it in the analysis of fuel economy. EWP can be calculated using equation (5), wherein WP_dual stands for work production capacity per unit price when the engine works in the dual fuel mode and

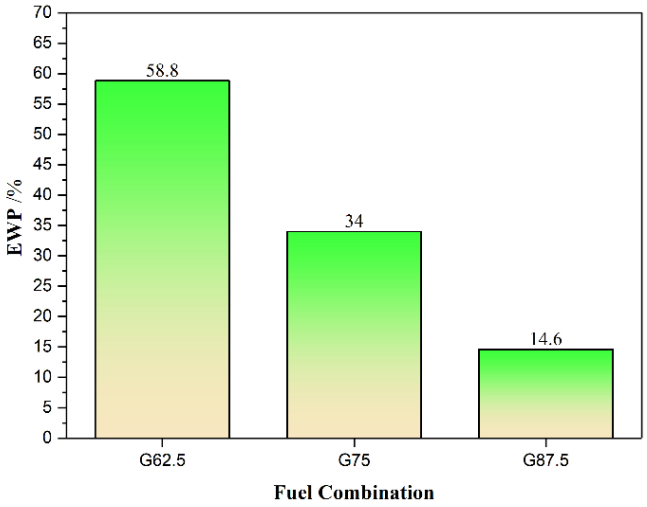

Fig. 9. EWP values in various gasoline-NG dual fuel modes

WP_G100 stands for work production capacity per unit price when the engine works in the gasoline-only mode.

$$EWP = \frac{(WP_{dual} - WP_{G100})}{WP_{G100}} \times 100 \quad \textbf{(5)}$$

Gasoline price in Iran is approximately 6.04 times higher than that of NG. That is why changing the design of SI engines in a way that they can work with dual fuel mixtures is a justifiable decision. Figure 9 shows EWP in the dual fuel modes under investigation. As can be seen, higher percentages of NG in the dual fuel mixture are associated with higher amounts of work per cycle. The amount of work per cycle in G62.5 mode has increased by 57.9% in comparison with that of the G100 mode. This indicates the superiority of gasoline-NG dual fuel mixtures over gasoline in terms of economic efficiency.

4. CONCLUSION

In this experimental study, the performance parameters of a single-cylinder research SI engine were analyzed in four different fuel modes (G100, G87.5, G75, and G62.5) at the compression ratio of 10, engine speed of 1800 rpm, and stoichiometric equivalence ratio. The results of the analysis of 400 consecutive cycles in each test are summarized below:

- In the present study, the entire range of spark advance at each mode was divided into 3 different parts: totally knocking limit (%KC>10), transitory or borderline limit (0<%KC<10), and totally non-knocking limit (%KC=0). Furthermore, the %KC of higher than 0 and lower than 5 was defined as the safe knock limit. Also, the maximum imep was used to determine the optimum spark advance in the safe knock limit. Each of the fuels in the dual fuel mixture has distinctive properties. That is why the efficiency of different fuel mixtures at optimum spark advances in the safe knock limit was assessed and compared at the same engine speed (1800 rpm) and equivalence ratio (stoichiometric). The analysis of the data revealed that in all of the dual fuel modes, maximum imep value was observed at optimum spark advances in totally non-knocking limit. In gasoline-only mode, however, maximum imep was observed in the safe knock limit. Moreover, in the G62.5 mode, the spark advance did not enter the totally knocking limit.
- The analysis of σ and COV in the imep of the fuel mixtures demonstrated that with the increase of NG percentage in the fuel mixture the values of both σ and COV reduced. In G62.5 mode, both of them reduced by 50% in comparison with the gasoline-only mode.
- Economic parameters were also assessed in this study and the results indicated that the cost of work per cycle decreased following the addition of NG to the fuel mixture. In G62.5 mode, the amount of the generated work per unit price was observed to be 58.8% higher than that of the gasoline-only mode.

REFERENCES

1. M. S. Lounici, M. A. Benbellil, K. Loubar, D. C. Niculescu, and M. Tazerout, “Knock characterization and development of a new knock indicator for dual-fuel engines,” Energy, vol. 141, pp. 2351-2361, 2017.
2. L. Chen, R. Zhang, H. Wei, and J. Pan, “Effect of flame speed on knocking characteristics for SI engine under critical knocking conditions,” Fuel, vol. 282, no. 118846, 2020.
3. N. Peters, B. Kerschgens and G. Paczko, “Super-knock prediction using a refined theory of turbulence,” SAE International Journal of Engines, vol. 6, no. 2, pp. 953-967, 2013.
4. L. Chen, R. Zhang, J. Pan, and H. Wei, “Optical study on autoignition and knocking characteristics of dual-fuel engine under CI vs SI combustion modes,” Fuel, vol. 266, pp. 107-117, 2020.
5. A. Kakaee, and A. Paykani, "Research and development of natural-gas fueled engines in Iran," Renewable and Sustainable Energy Reviews, vol. 26: pp. 805-821, 2013.
6. RJ. Nichols, “The challenges of change in the auto industry: why alternative fuels?,” Journal of Engineering for Gas Turbines and Power Print, vol. 116, no. 4, pp. 727-732. 1994.
7. H. M. Cho, H. Bang-Quan, “Spark ignition natural gas engines – a review,” Energy Conversion and Management, vol. 48, no. 2, pp. 608–618, 2007.
8. D. Feng, H. Wei, M. Pan, L. Zhou, and J. Hua, “Combustion performance of dual-injection using n-butanol direct-injection and gasoline port fuel-injection in a SI engine,” Energy, vol. 160, pp. 573-581, 2018.
9. H. Liu, Z. Wang, and J. Wang, “Methanol-gasoline DFSI (dual-fuel spark ignition) combustion with dual-injection for engine knock suppression,” Energy, vol. 73, pp. 686-693, 2014.
10. E. Pipitone, S. Beccari. “Performances improvement of a S.I. CNG bi-fuel engine by means of double-fuel injection,” SAE Technical Paper; vol. 24, no. 0058, pp. 78-86, 2009.
11. M. Movahed, H. Tabrizi, M. Mirsalim, “Experimental investigation of the concomitant injection of gasoline and CNG in a turbocharged spark ignition engine,” Energy conversion and management, vol. 80, pp. 126-136, 2014.
12. D. Ramasamy, C. Y. Goh, K. Kadirgama, F. Benedict, M. Noor, G. Najafi and A. P. Carlucci, “Engine performance, exhaust emission and combustion analysis of a 4-stroke spark ignited engine using dual fuel injection,” Fuel, vol. 207, pp. 719-728, 2017.
13. M. Sarabi, E. Abdi Aghdam, “Experimental analysis of in-cylinder combustion characteristics and exhaust gas emissions of gasoline–natural gas dual-fuel combinations in a SI engine,” Journal of Thermal Analysis and Calorimetry, vol. 139, no. 5, pp. 3165-3178, 2020.
14. M. Sarabi, E. Abdi Aghdam, “Single-Cylinder SI Engine Performance in Dual-Fuel (Gasoline-NG) Mode with Gasoline Dominant Fuel under Stoichiometric Conditions,” Modares Mechanical Engineering, Vol. 20, no. 2, pp. 287-295, 2020.
15. A. Karvountzis-Kontakiotis, H. Vafamehr, A. Cairns, and M. Peckham, “Study on pollutants formation under knocking combustion conditions using an optical single cylinder SI research engine,” Energy, vol. 158, pp. 899-910, 2018.
16. R. B. R. da Costa, J. J. Hernández, A. F. Teixeira, N. A. D. Netto, R. M.

Valle, V. R. Roso, and C. J. Coronado, “Combustion, performance and emission analysis of a natural gas-hydrous ethanol dual-fuel spark ignition engine with internal exhaust gas recirculation,” Energy Conversion and Management, vol. 195, pp. 1187-1198, 2019.
17. E. Abdi Aghdam, M. Bashi, “Effectiveness of performance characters of a SI engine by varying injection start position of gasoline and natural gas fuels,” Modares Mechanical Engineering, Vol. 15, no. 8, pp. 134-42, 2015.
18. E. Abdi Aghdam, M. ghorbanzade, “The effect of different fuels (gasoline & natural gas) on cyclic variations of a spark ignition engine running on lean mixture,” Modares Mechanical Engineering, Vol. 13, no. 12, pp. 101-108, 2014.
19. M. Sarabi, E. Abdi Aghdam, S.K. Yekani, “The Effect of Burned Residual Gases on Gasoline-NG Dual-Fuel Engine Combustion Performance with Skip-Fire Technique,” The Journal of Engine Research, vol. 63, no. 63, pp. 3-11, 2021.
20. E. Abdi Aghdam, M. Sarabi, “Calibration of Gasoline-NG Dual-Fuel SI Engine Injectors and Comparison of the Performance and Emission of a Dual-Fuel and Single Fuel Cases,” Journal of Mechanical Engineering, Vol. 52, no. 1, pp. 109-117, 2021.
21. E. Abdi Aghdam, M. Sarabi, M. Mehrbod Khomeyrani, “Experimental study of laminar burning velocity for dual fuel (Gasoline-NG)-Air mixture using pressure record in a spherical combustion bomb at higher primary pressure,” Fuel and Combustion, Vol. 11, no. 1, pp. 121-34. 2018.
22. J. B. HEYWOOD, “Internal combustion engine fundamentals,” Mcgraw-hill New York, 1988.
23. F. Amrouche, P. Erickso, S. Varnhagen, J.W. Park, “An experimental analysis of hydrogen enrichment on combustion characteristics of a gasoline Wankel engine at full load and lean burn regime,” International Journal of Hydrogen Energy, vol. 43, no. 41, pp. 19250-19259, 2018.
24. D. Xiongbo, L. Yangyang, L. Jingping, G. Genmiao, F. Jianqin, “Experimental study the effects of various compression ratios and spark timing on performance and emission of a lean-burn heavy-duty spark ignition engine fueled with methane gas and hydrogen blends,” Energy, vol. 169, pp. 558-571, 2018.
25. E. Abdi Aghdam E, M. Ataee Tarzanagh, “The Effect of Burned Residual Gases on Optimum Ignition Timing using Skip Fire Technique,” The Journal of Engine Research, vol. 50, no. 50, pp. 67-75, 2018.
26. M. Ceviz, A. Sen, A. Ku¨leri ,IV. O¨ ner, “Engine performance, exhaust emissions, and cyclic variations in a lean-burn SI engine fueled by gasoline–hydrogen blends,” Applied Thermal Engineering, vol. 36, pp. 314-324, 2012.